Article

A New State of Charge Estimation Method for LiFePO₄ Battery Packs Used in Robots

Ming-Hui Chang [1], Han-Pang Huang [1],* and Shu-Wei Chang [2]

[1] Department of Mechanical Engineering, National Taiwan University, Taipei 10617, Taiwan;
E-Mail: d93522037@ntu.edu.tw

[2] Graduate Institute of Industrial Engineering, National Taiwan University, Taipei 10617, Taiwan;
E-Mail: r99546045@ntu.edu.tw

* Author to whom correspondence should be addressed; E-Mail: hanpang@ntu.edu.tw;
Tel.: +886-2-33664478; Fax: +886-2-23676064.

Abstract: The accurate state of charge (SOC) estimation of the LiFePO₄ battery packs used in robot applications is required for better battery life cycle, performance, reliability, and economic issues. In this paper, a new SOC estimation method, "Modified ECE + EKF", is proposed. The method is the combination of the modified Equivalent Coulombic Efficiency (ECE) method and the Extended Kalman Filter (EKF) method. It is based on the zero-state hysteresis battery model, and adopts the EKF method to correct the initial value used in the Ah counting method. Experimental results show that the proposed technique is superior to the traditional techniques, such as ECE + EKF and ECE + Unscented Kalman Filter (UKF), and the accuracy of estimation is within 1%.

Keywords: equivalent coulombic efficiency (ECE); extended Kalman filter (EKF); LiFePO₄; state of charge (SOC) estimation

1. Introduction

In recent years, interest has increased significantly in the use of lithium ion (Li-ion) batteries for some applications, such as hybrid electric vehicles (HEVs), battery electric vehicles (BEVs), plug-in hybrid electric vehicles (PHEVs), and robotic systems. The features of light weight, high energy density, high galvanic potential, and long life cycle of Li-Ion are superior to either lead-acid or

nickel-metal hydride batteries, as their energy and power have been remarkably extended to achieve the high traction power and long lifetime required in these applications. In real-world use, accurate information of the state of charge (SOC) of a robot's battery packs is required for a good battery management system.

SOC is generally defined as the ratio of standard remaining capacity to the nominal capacity:

$$SOC(t) = SOC(t_0) - \int_0^t \frac{\eta I(t)}{C} dt \tag{1}$$

where $SOC(t)$ is the SOC at time instant t; $SOC(t_0)$ is the initial value; C is the nominal capacity; and $I(t)$ is the current at time t. The current is positive during the discharging process and negative during the charging process. In general, $\eta = 1$ for discharge and $\eta < 1$ for charge under standard conditions with a constant $C/3$ rate. As the current rate is usually quite variable in real situations, ECE (introduced in Section 2) has been developed to measure the energy loss.

Failure to estimate SOC accurately can easily cause over-discharging or over-charging situations, resulting in a decreased capability to yield power as well as decreased battery pack longevity. For this reason, accurate SOC estimation is considered very important for robot applications. Several methods of estimating the SOC have been developed, e.g., the Ah counting approach [1,2], the Equivalent Coulombic Efficiency (ECE) approach [1,3], Open-Circuit Voltage (OCV) measurements [4], the Dynamic Equivalent Circuit-based Model (DECM) [5–12], the Electrochemical Impedance Spectroscopy (EIS) approach [13–15], the Electromotive Force (EMF) approach [16], the Fuzzy Logic approach [17], the Artificial Neural Network (ANN) approach [18], the Support Vector Machine (SVM) method [19], and the Kalman Filtering approach [20]. Non-linear Kalman filters, such as the Extended Kalman filter (EKF) [21–27], the Dual Extended Kalman filter (DEKF) [4], the Unscented Kalman Filter (UKF) [28–31], the Adaptive Extended Kalman Filter (AKEF) [32,33], and the Adaptive Unscented Kalman Filter (AUKF) [34], have been developed.

According to the choice of battery model, the SOC estimation methods can be approximately categorized into three major types [9]. The first type is the non-model-based coulomb counting method applied to many BEV/HEV BMSs and battery storage simulations. This online sampling approach is the straightforward application of Equation (1). The battery packs' current is measured constantly and used to update the SOC. If the current is measured accurately, implementation is inexpensive and reliable, though the method has several drawbacks [1]. Firstly, it cannot determine the initial SOC. Secondly, it is difficult to measure coulombic efficiency correctly. Thirdly, the error is larger when the battery works at low or high temperatures. Finally, in practice, the open-loop algorithm often results in the accumulation of measurement errors due to uncertain disturbances. This means that regular recalibration is required, a difficult procedure to be implemented in the highly dynamic operations of the electrical system. To solve these problems, the Ah counting approach is combined with the Peukert equation [35] to calculate the coulombic efficiency. This quantity, however, is not only a function of current but is also affected by SOC and temperature. Therefore, the combination of the two approaches has not yielded a reliable result.

The second category of SOC estimation methods uses black-box battery models that describe the nonlinear relationship between the SOC and its influencing factors. Based on principles like ANN, fuzzy logic optimization, and SVM, these models are often established by computational intelligence-based

approaches. Given an appropriate training data set, they can provide good SOC estimation through their abilities to approximate nonlinear function surfaces. However, there are two drawbacks. One is that the learning process imposes a heavy computational load, so most SOC estimation models of this type are used offline. The other is that good performance is achievable only if sufficient and reliable training data are available. Both these problems can lead to poor robustness under certain battery operating conditions.

The third category is based on Kalman filtering techniques using state-space battery models and is favored because it is closed loop (self-corrected), online, and offers a dynamic SOC estimation error range. This category is most suitable for real-time battery management and electrical system control.

In this paper, a new and highly precise SOC estimation method, called "Modified ECE + EKF" method, is proposed. It combines a modified ECE method, which considers self-discharge and the influence of temperature and SOC on the coulombic efficiency, with an EKF-based method that makes the approximate initial SOC value converge to its real value. In addition, a battery model suitable for real-time implementation is also proposed. It consists of two parts. The first is an adaptation of the "combined model," describing the relationship between OCV and SOC, that performs better than any one of the Shepherd, Unnewehr, or Nernst models [36]. The second part is a zero-state hysteresis correction term. Based on a linear discrete-time model form, a least-square algorithm is used to estimate the parameters of the model. The proposed SOC estimation method will be demonstrated using two experimental tests. A comparison of algorithms among Modified ECE + EKF, ECE + EKF, and ECE + UKF show that the proposed SOC estimation method has better accuracy.

The remainder of this paper is organized as follows: the measurement and modification of the ECE method are introduced in Section 2, and a description of the structure and parameterization of the zero-state hysteresis battery model is given in Section 3. Section 4 presents the EKF-based SOC estimation algorithm, and Section 5 discusses two experiments to validate the proposed method and compare the method with the ECE + EKF and ECE + UKF estimation approaches. Section 6 shows an application in robots to justify the accuracy and robustness of the proposed algorithm. Finally, our conclusions are summarized in Section 7.

2. Equivalent Coulombic Efficiency (ECE)

The coulombic efficiency of battery packs is defined as the ratio of the discharged capacity to the capacity needed to be charged to the initial state before discharge and it can be calculated as:

$$\eta = \int_0^{t_d} I_d dt \bigg/ \int_0^{t_c} I_c dt \qquad (2)$$

where I_d is the discharging current; t_d is the discharging time; I_c is the charging current; and t_c is the charging time.

The coulombic efficiency, shown in Equation (2), is the ratio of the discharging capacity to the charging capacity. It varies according to current rate, and hence an accurate SOC estimation depends on accurate calculation of both charge and discharge coulombic efficiency.

2.1. Calculation of the Equivalent Coulombic Efficiency

To calculate the charge and discharge coulombic efficiency of a robot's battery packs, the ECE measurement method [37] is adopted in this paper, and we use "2S8P × 4" LiFePO₄ battery packs as a test sample to calculate the ECE, as shown in Figure 1. Here, "2S8P × 4" indicates that each pack has four "2S8P" battery packs in series, each with a nominal capacity of 8.4 Ah.

Figure 1. LiFePO₄ battery packs (2S8P × 4).

As the coulombic efficiency is different at different currents, the *C*/3 rate is used as the base current to define the base coulombic efficiency and the ECE when batteries are charged or discharged. The base coulombic efficiency can be calculated by Equation (3) after completing the following procedure:

(1) Discharge at the *C*/3 rate until the terminal voltage limit is reached;
(2) Charge at the *C*/3 rate until *SOC* = 1 and the charging capacity is Q_{CB};
(3) Rest the battery pack for 5 min until it is in the balanced state;
(4) Discharge at the *C*/3 rate until the terminal voltage limit is reached. The discharging capacity is Q_{DB}.

The base coulombic efficiency of LiFePO₄ battery packs can then be calculated as:

$$\eta_{C/3} = Q_{DB}/Q_{CB}$$
(3)

However, in this paper, the equivalent charge coulombic efficiency of LiFePO₄ battery packs is calculated by Equation (4) after completing the following procedure:

(1) Discharge at the *C*/3 rate until terminal voltage limit is reached;
(2) Charge at several different currents I_C (*C*/3, *C*/2, 1*C*, 1.5*C*, 2*C*, 2.5*C*) until *SOC* = 1. The charging capacity is $Q_{CC} = I_C \cdot t_{CC}$, where t_{CC} is the charging time. This step will keep the current constant at different values in different charge cycles. Therefore, we finally have six charge cycles;
(3) Rest the battery pack for 5 minutes until it is in a balanced state;
(4) Discharge at the *C*/3 rate until the terminal voltage limit is reached. The discharging capacity is $Q_{DC} = (C/3) \cdot t_{DC}$, where t_{DC} is the discharging time.

The equivalent charge coulombic efficiency of LiFePO₄ battery packs can then be calculated as:

$$\eta_C = Q_{DC} \bigg/ Q_{CC} = \left(\frac{C}{3} \cdot t_{DC}\right) \bigg/ \left(\sum I_C \cdot t_{CC}\right)$$
(4)

In addition, the equivalent discharge coulombic efficiency of LiFePO$_4$ battery packs is calculated by Equation (5) after completing the following procedure:

(1) Discharge at a specific current until the terminal voltage limit is reached;
(2) Charge at the *C*/3 rate until *SOC* = 1. The discharging capacity is $Q_{CD} = (C/3) \cdot t_{CD}$, where t_{CD} is the charging time;
(3) Rest the battery pack for 5 minutes until it is in a steady state;
(4) Discharge at several different currents I_D (*C*/3, *C*/2, 1*C*, 1.5*C*, 2*C*, 2.5*C*) until the terminal voltage limit is reached. The discharging capacity is $Q_{DD} = I_D \cdot t_{DD}$, where t_{DD} is the discharging time. This step will keep the current constant at different values in different discharge cycles. Therefore, we finally have six discharge cycles.

The equivalent discharge coulombic efficiency of LiFePO$_4$ battery packs can then be calculated as:

$$\eta_D = Q_{DD} \Big/ Q_{CD} = \left(\sum I_D \cdot t_{DD}\right) \Big/ \left(\frac{C}{3} \cdot t_{CD}\right) \tag{5}$$

Figure 2 shows the calculated equivalent charge and discharge coulombic efficiency of LiFePO$_4$ battery packs, and the base coulombic efficiency $\eta_{C/3} = 0.9982$. To calculate these results conveniently, a linear fitting method is used to fit the equivalent coulombic efficiency.

Figure 2. Equivalent charge and discharge coulombic efficiency of LiFePO$_4$ battery packs.
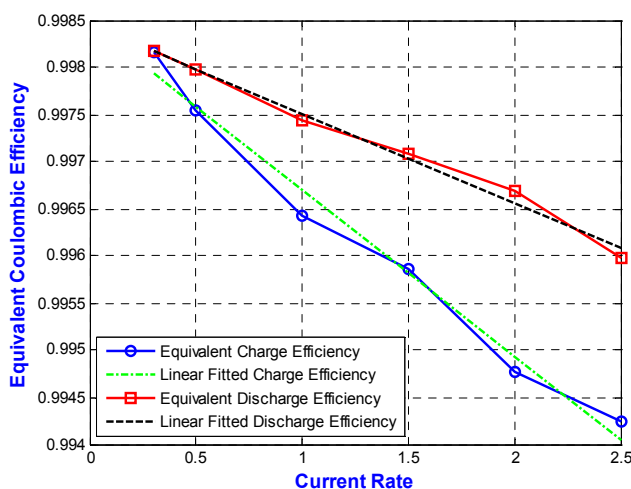
2.2. Modified ECE Method

The charging and discharging processes for different current rates can be converted into a single process for constant current. Let Q_0 be the initial capacity. Q_{CN} is the charging capacity at current I_{CN}; where $Q_{CN} = I_{CN} \cdot t_{CN}$; and t_{CN} is the charging time; Q_{DN} is the discharging capacity at current I_{DN}; where $Q_{DN} = I_{DN} \cdot t_{DN}$; and t_{DN} is the discharging time. The equivalent charging capacity Q_C and its discharging capacity Q_D are calculated by Equations (6) and (7), respectively:

$$Q_C = \frac{Q_{CN}}{\eta_{C/3}} \eta_C = \frac{I_{CN} t_{CN}}{\eta_{C/3}} \eta_C \tag{6}$$

$$Q_D = \frac{Q_{DN}}{\eta_D}\eta_{C/3} = \frac{I_{DN}t_{DN}}{\eta_D}\eta_{C/3} \tag{7}$$

In the entire operating process of the battery packs, the practical consumed capacity Q_T at room temperature under the actual discharge/charge rate is calculated by Equation (8). The baselines of each term in Equation (8) are all with $C/3$ rate:

$$Q_T = Q_0 + \sum Q_C\eta_{C/3} - \sum Q_D = Q_0 + \sum I_{CN}t_{CN}\eta_C - \sum \frac{I_{DN}t_{DN}}{\eta_D}\eta_{C/3} \tag{8}$$

The coulombic efficiency in the low (capacity <12 Ah) and high (capacity >76 Ah) SOC ranges is smaller than that in the normal SOC range (SOC = 0.2–0.8). For electrical systems, the designed coulombic efficiency is usually between 0.94 and 0.98 in the normal SOC range [1]. In this paper, the coefficient K_S is defined to modify the influence of the SOC on the coulombic efficiency. In the normal SOC range, base coulombic efficiency does not vary significantly, so the value of K_S is set to 0.98 in this paper.

Figure 3 shows the influence of temperature on coulombic efficiency. The battery pack is charged and discharged at the $C/3$ rate under different temperatures (45, 25, 0, and −10 °C), respectively [14]. The test indicates that temperature influences the coulombic efficiency, and that the relationship between efficiency and temperature is non-linear, as shown in Table 1. In this paper, the coefficient K_T is defined to modify the influence of temperature on coulombic efficiency.

Figure 3. The influence of temperature on coulombic efficiency.
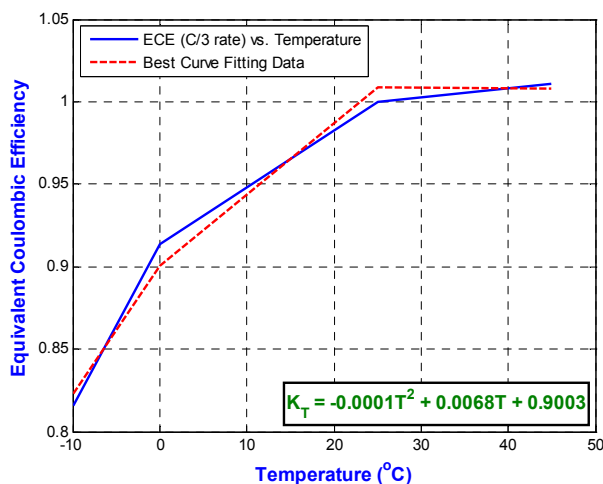
Table 1. The relationship between efficiency and temperature.

Temperature (°C)	K_T
−10	0.8154
0	0.9134
25	1
45	1.0107

Any battery will lose energy through self-discharge, a phenomenon in which internal chemical reactions continuously reduce the stored charge, even when the battery is disconnected. When it is

connected, its internal resistance also consumes energy. Both of these unavoidable losses of available energy must be taken into account when considering the charging-discharging process. Self-discharge decreases the shelf life of battery packs so that they are not fully charged on first use. The higher the environmental temperature is, the larger the self-discharge will be. It also affects the SOC estimation accuracy significantly. Self-discharge of LiFePO$_4$ battery packs is typically less than 3% per month, so the effect is very small for periods of a day or so. It becomes more significant for longer periods between charging, and can be the source of accumulating errors unless the battery monitoring circuit is regularly reset or calibrated. The self-discharge coefficient K_{SD} is therefore set to 2×10^{-8} in this paper.

If a battery is left to relax after charging or discharging, it takes some time for the terminal voltage to reach the new steady state value. This is called *relaxation effect*, and for low discharge/charge rates it can be mitigated to a certain extent through battery relaxation. Although the relaxation model's behavior is similar to the behavior of commercial batteries, there is considerable difficulty in its implementation, since the relaxation effect involves many physical and electrochemical properties of the battery [8].

To overcome these problems, a modified ECE method that considers self-discharge, influence of temperature and SOC on the coulombic efficiency (but not the relaxation effect) is proposed as follows:

$$Q_T = Q_0 - Q_{SD} + \sum Q_C \eta_{C/3} - \sum Q_D = Q_0 - \sum K_{SD} C \Delta t + \sum K_S K_T I_{CN} t_{CN} \eta_C - \sum \frac{I_{DN} t_{DN}}{\eta_D} K_S K_T \eta_{C/3} \tag{9}$$

where Q_{SD} is the self-discharge quantity of battery packs and Δt is the sample interval whose value is 1 second.

The modified SOC is now defined as:

$$SOC(t) = \frac{Q_T}{C} \tag{10}$$

3. Battery Modeling

In this paper, the zero-state hysteresis [24,32,34] battery model is used as the battery packs model, which is often applied to the Kalman filter-based SOC estimation. Equations (11,12) represent the zero-state hysteresis model:

$$s_{k+1} = f(s_k, i_k) + w_k = s_k - \left(\frac{\eta_k \cdot \Delta t}{C}\right) i_k + w_k \tag{11}$$

$$y_k = g(s_k, i_k) + v_k = OCV(s_k) - i_k R - h_k H + v_k \tag{12}$$

where s is the SOC to be determined; i is the battery packs' current and is indicated positive under discharge and negative under charge; y is the battery packs' terminal voltage; Δt is the sample interval; and k is the time step index; R is the battery packs' internal resistance; The parameters w and v are independent and zero-mean Gaussian noises for the process and measurement, and their covariance values are Q_w and R_v, respectively; H is the hysteresis value; and h is a function of the sign of the current:

$$h_k = \begin{cases} 1, & i_k > \varepsilon \\ -1, & i_k < -\varepsilon \\ h_{k-1}, |i_k| \le \varepsilon \end{cases} \tag{13}$$

where ε is a small positive value. In Equation (13), the first case is in the discharging process, the second case is in the charging process, and the final situation is in the rest mode.

The function $OCV(s_k)$, the open-circuit voltage as a function of the SOC, can be calculated as:

$$OCV(s_k) = K_0 - \frac{K_1}{s_k} - K_2 s_k + K_3 \ln(s_k) + K_4 \ln(1 - s_k) \tag{14}$$

where K_0, K_1, K_2, K_3, and K_4 are the fitting coefficients chosen to make the model fit the data well. They are used to describe the battery packs' OCV.

4. EKF Algorithm Based on the Battery Model

For the non-linear battery packs model considered in this paper, the extended Kalman filter is combined with the modified ECE method to estimate the SOC of LiFePO$_4$ battery packs. The EKF is widely used in estimation problems, as it often works very well although it is not necessarily optimal. To apply the EKF, the non-linear battery packs model in Equations (11,12) are made linear by a first-order Taylor-series expansion, assuming that $f(\cdot,\cdot)$ and $g(\cdot,\cdot)$ are differentiable at all operating points (s_k, i_k). The linear models are then obtained as Equations (15,16):

$$s_{k+1} = A_k s_k + f(\hat{s}_k, i_k) - A_k \hat{s}_k + w_k \tag{15}$$

$$y_k = C_k s_k + g(\hat{s}_k, i_k) - C_k \hat{s}_k + v_k \tag{16}$$

where A_k and C_k are defined as:

$$A_k = \left. \frac{\partial f(s_k, i_k)}{\partial s_k} \right|_{s_k = \hat{s}_k} \tag{17}$$

$$C_k = \left. \frac{\partial g(s_k, i_k)}{\partial s_k} \right|_{s_k = \hat{s}_k} \tag{18}$$

The discrete-time state function is given by applying Equations (9,10) into Equation (11):

$$s_{k+1} = \begin{cases} s_k - K_{SD} - i_k \Delta t K_S K_T \eta_C / C + w_k, & i_k < 0 \\ s_k - K_{SD} - i_k \Delta t K_S K_T \dfrac{\eta_{C/3}}{\eta_D} \Big/ C + w_k, & i_k > 0 \end{cases} \tag{19}$$

The combined discrete-time model based measurement function can be obtained by substituting Equation (14) into Equation (12):

$$y_k = K_0 - i_k R - \frac{K_1}{s_k} - K_2 s_k + K_3 \ln(s_k) + K_4 \ln(1 - s_k) - h_k H + v_k \tag{20}$$

Based on the nonlinear discrete-time state-space battery packs model in Equations (19) and (20), the prediction and correction processes of the EKF combined with modified ECE method are described as follows:

(1) Given an initial SOC estimate $\hat{s}_0$, initial covariance matrix Cov_0 and noise parameters;

(2) After sampling the terminal voltage y_k and current i_k of the battery packs for sampling time $k = 1, 2, 3\ldots$, the calculation processes are iterated as follows:

State (SOC) estimate update:

$$\hat{s}_{k/k-1} = \begin{cases} \hat{s}_{k-1/k-1} - K_{SD} - i_k \Delta t K_S K_T \eta_C / C + w_k, & i_k < 0 \\ \hat{s}_{k-1/k-1} - K_{SD} - i_k \Delta t K_S K_T \dfrac{\eta_{C/3}}{\eta_D} \Big/ C + w_k, & i_k > 0 \end{cases} \tag{21}$$

Error covariance update:

$$Cov_{k/k-1} = Cov_{k-1/k-1} = A_k Cov_{k-1/k-1} A_k^T + Q_w \tag{22}$$

Kalman gain matrix calculation:

$$L_k = Cov_{k/k-1} \hat{C}_k^T \left[\hat{C}_k Cov_{k/k-1} \hat{C}_k^T + R_v \right]^{-1} \tag{23}$$

where $\hat{C}_k$ is defined as:

$$\hat{C}_k = \left. \frac{\partial g(s_k, i_k)}{\partial s_k} \right|_{s_k = \hat{s}_{k/k-1}} = K_1 / \left(\hat{s}_{k/k-1} \right)^2 - K_2 + K_3 / \hat{s}_{k/k-1} - K_4 / \left(1 - \hat{s}_{k/k-1} \right) \tag{24}$$

SOC estimate measurement update:

$$\hat{s}_{k/k} = \hat{s}_{k/k-1} + L_k \left[y_k - g\left(\hat{s}_{k/k-1}, i_k \right) \right] \tag{25}$$

Error covariance measurement update:

$$Cov_{k/k} = \left(I - L_k \hat{C}_k \right) Cov_{k/k-1} \tag{26}$$

(3) The prediction and correction processes repeat for every time step until the initial SOC estimation has converged to its real value.

The modified ECE + EKF algorithm realized with the prediction and correction processes is clearly shown in Figure 4 [2,32].

Figure 4. The operation of EKF.

Time Update (Prediction)

(1) *Predict the SOC :*

$$\hat{s}_{k/k-1} = \begin{cases} \hat{s}_{k-1/k-1} - K_{SD} - i_k \Delta t K_S K_T \eta_C / C + w_k, & i_k < 0 \\ \hat{s}_{k-1/k-1} - K_{SD} - i_k \Delta t K_S K_T \dfrac{\eta_{C/3}}{\eta_D} \bigg/ C + w_k, & i_k > 0 \end{cases}$$

(2) *Predict the error covariance :*

$$Cov_{k/k-1} = A_k Cov_{k-1/k-1} A_k^T + Q_w$$

Measurement Update (Correction)

(3) *Compute the Kalman Gain :*

$$L_k = Cov_{k/k-1} \hat{C}_k^T \left[\hat{C}_k Cov_{k/k-1} \hat{C}_k^T + R_v \right]^{-1}$$

(4) *Correct the SOC with measurement :*

$$\hat{s}_{k/k} = \hat{s}_{k/k-1} + L_k \left[y_k - g\left(\hat{s}_{k/k-1}, i_k \right) \right]$$

(5) *Correct the error covariance with measurement :*

$$Cov_{k/k} = \left(I - L_k \hat{C}_k \right) Cov_{k/k-1}$$

initial estimates for $\hat{s}_0$ *and* Cov_0

5. Experimental Results

5.1. Battery Test Bench

Battery pack tests are performed to identify the model parameters. As shown in Figure 5, the experimental setup consists of a power battery production equipment set (MCF-60L2030A), a scanner box (ES-100A), two communication conversion boxes (CNB-1004A) and a LabVIEW-based virtual measurement unit.

Figure 5. Schematic diagram of the battery pack test bench.
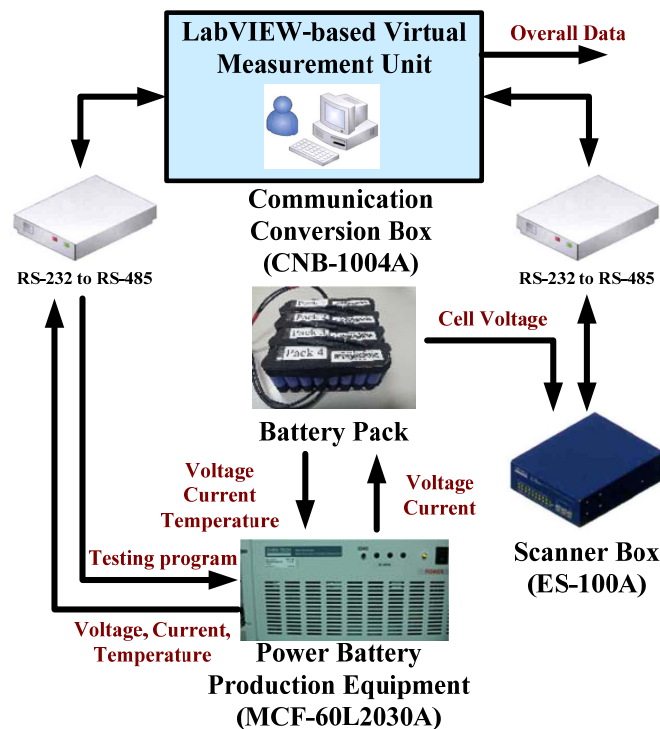
The MCF-60L2030A test equipment, supplied by Chen Tech Technology (CTT, New Taipei, Taiwan), provides flexibility for loading the battery, designed for 60 V maximum voltage, 20 A maximum charging current, and 30 A maximum discharging current. The recorded data include time, load current, terminal voltage, temperature, and accumulative Amp-hours (Ah), and Watt-hours (Wh). The sampling time and safety start/stop criteria can be defined separately. The CNB-1004A is a RS-232 to RS-485 conversion box. The measured voltage, current, and temperature are transmitted through the CNB-1004A to the LabVIEW-based virtual measurement unit. The errors of the voltage and current sensors are less than 0.02% and 0.03%, respectively. The ES-100A can collect the voltage of each cell in the battery and transmit it to the LabVIEW-based virtual measurement unit through the CNB-1004A, driven by the LabVIEW program. The experimental results of two case studies given below are used to verify the proposed method. The average temperatures of two experiments are listed in Table 2.

Table 2. The average temperature of the two experiments.

Temperature (°C)	Experiment I	Experiment II	
		Discharge	Charge
The test begins	26.44	26.41	24.8
The test ends	23.2	21.91	24.6

5.2. Experiment I: Under Fixed Constant-Current Pulse Conditions

We set up Experiment I to estimate the SOC of LiFePO$_4$ battery packs when the SOC state is correctly initialized to 100%. The experiments include seven discharges and six charges under fixed constant-current pulse conditions. The current and voltage profiles for Experiment I are shown in Figure 6a,b, respectively. The SOC value is an Ah counting method calculated by the LabVIEW-based virtual measurement unit, where accurate initial SOC is given and the coulombic efficiency is considered, as shown in Figure 6c.

Figure 6. Identification test in experiment I. (**a**) Current profile; (**b**) Voltage profile; (**c**) SOC profile.

(**a**)

(**b**)
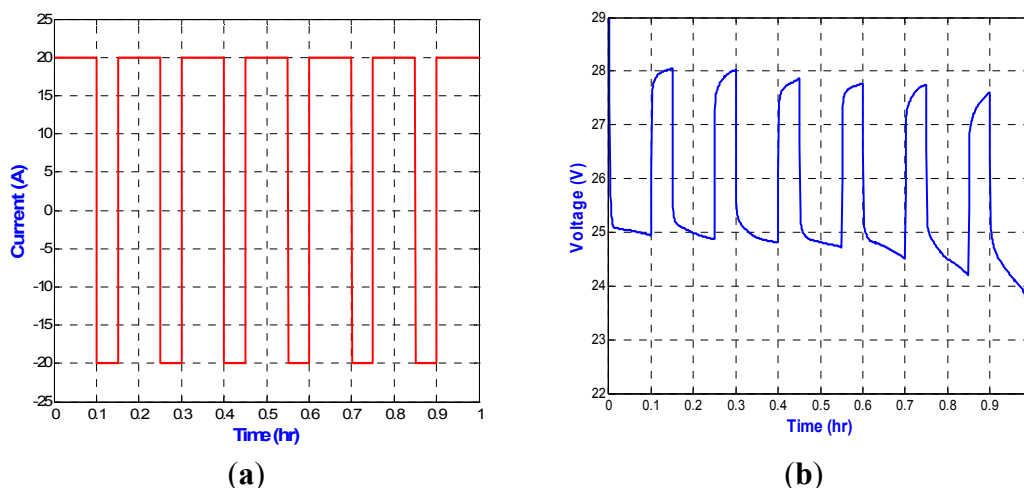
Figure 6. *Cont.*
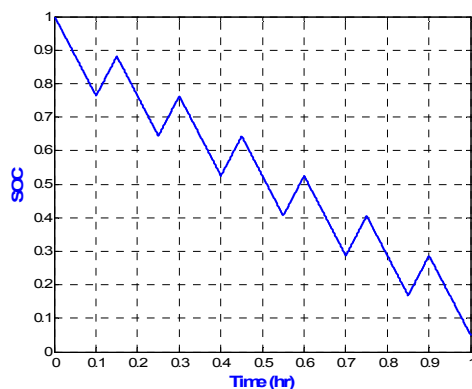
(c)

First, the battery pack is discharged at about 2.5*C* current (20 A in this case) for 6 minutes and data recorded at 1 second per point. The battery pack is then charged at about 2.5*C* current (−20 A in this case—in this paper, discharging current is taken as positive, charging current as negative) for 3 min and data recorded at 1 s per point. The cycle is repeated for 1 h.

In this paper, discharging current is taken as positive, charging current as negative, so Experiment I covers both discharging and charging processes. The general descending trend of battery voltage indicates that the test mainly discharges the battery.

5.3. Experiment II: Under Different Constant-current Pulse Test

In Experiment II, we set up two different current profiles to estimate the SOC of LiFePO$_4$ battery packs when the initial SOC is set to 0.5, as shown in Figure 7a,b, respectively. For each type of current profile, the battery pack is discharged or charged based on the constant-current pulse and rest sequences. The battery pack is discharged and charged from 20 A down to 2 A. The battery packs' terminal voltages decreased with the discharging, and increased with the charging current profiles. The terminal voltage profiles for Experiment II are shown in Figure 8a,b, respectively. The SOC profiles, calculated by the LabVIEW-based virtual measurement unit and based on the discharging and charging current profiles, are shown in Figure 9a,b, respectively.

Figure 7. Current profiles in experiment II. (**a**) Discharge; (**b**) Charge.

(a)

(b)
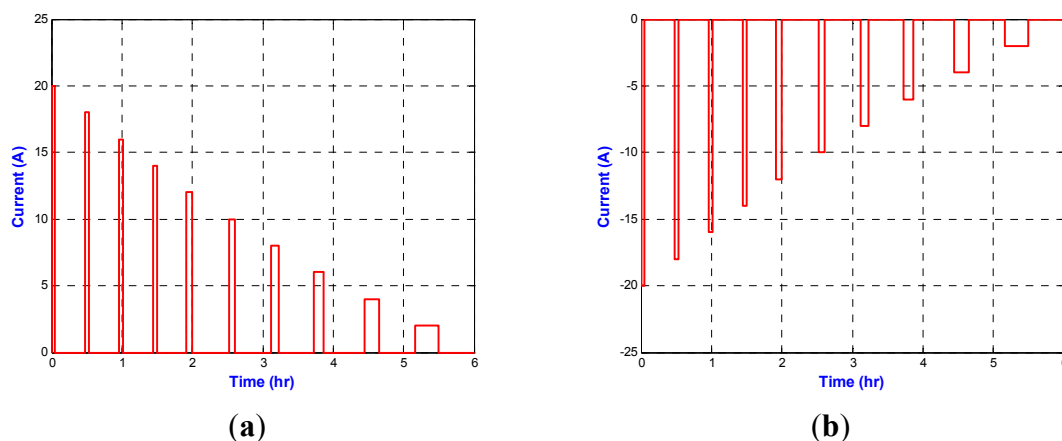
Figure 8. Voltage profiles in experiment II. (**a**) Discharge; (**b**) Charge.

(**a**) (**b**)
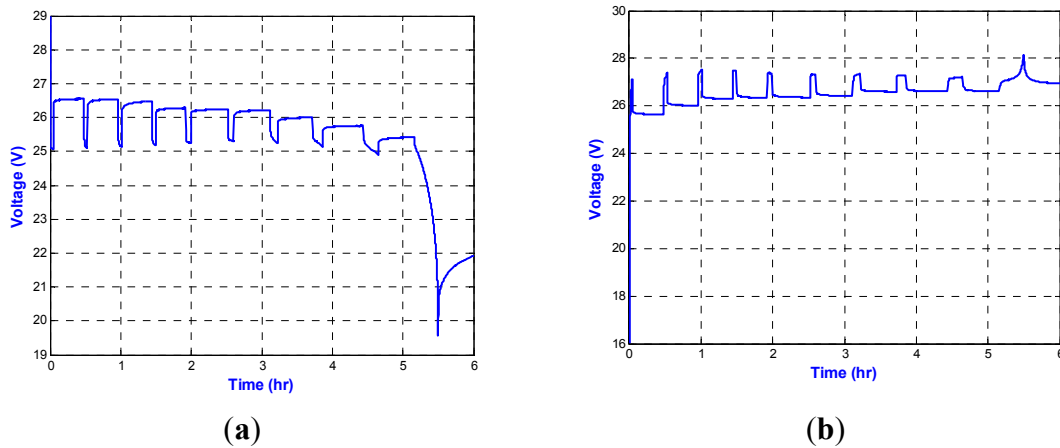
Figure 9. SOC profiles in experiment II. (**a**) Discharge; (**b**) Charge.

(**a**) (**b**)
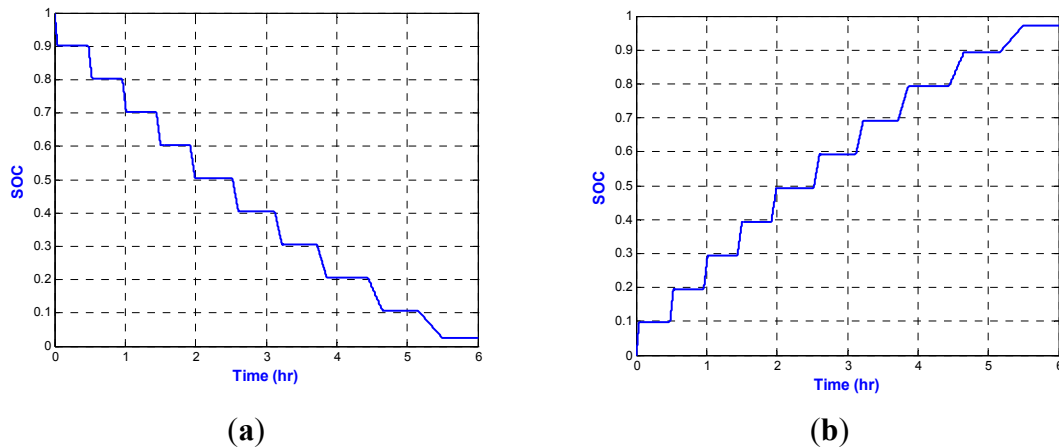
5.4. Model Parameter Identification

Given a set of samples, including the current, the terminal voltage and experimental SOC values of the battery packs, the modeling parameters of the battery packs can be determined by using the least square method. The output equation of the battery model is represented by a regression model, as expressed by:

$$
\begin{aligned}
y_k &= K_0 - \frac{K_1}{s_k} - K_2 s_k + K_3 \ln(s_k) + K_4 \ln(1-s_k) - i_k R - h_k H \\
&= \begin{bmatrix} 1 & -1/s_k & -s_k & \ln(s_k) & \ln(1-s_k) & -i_k^+ & -i_k^- & -h_k \end{bmatrix} \cdot \begin{bmatrix} K_0 & K_1 & K_2 & K_3 & K_4 & R^+ & R^- & H \end{bmatrix} \\
&= m_k^T \theta
\end{aligned}
\tag{27}
$$

where i_k^+ and i_k^- denote the discharging and charging currents, respectively. During the discharging process ($i_k > 0$), i_k^+ is equal to i_k and i_k^- is equal to 0. During the charging process ($i_k < 0$), i_k^+ is equal to 0 and i_k^- is equal to i_k. Similarly; R^+ and R^- are used to represent the internal resistance value under discharge and charge, respectively. For N number of observations, the output terminal voltage sequence, $\mathbf{Y} = [y_1, y_2, \ldots, y_N]^T$, can be written as:

$$
\mathbf{Y} = \mathbf{M}\theta
\tag{28}
$$

where $\mathbf{M} = [m_1, m_2,\ldots, m_N]^T$ is repressor matrix. As a result, the parameters can be obtained from $\boldsymbol{\theta} = (\mathbf{M}^T\mathbf{M})^{-1}\mathbf{M}^T\mathbf{Y}$ for a nonsingular $(\mathbf{M}^T\mathbf{M})$. To determine parameters, each observation in which the current is not zero is considered, because the zero-state hysteresis model cannot represent the slow variation of the time constant effect when the battery current is zero. The identified model parameters of the two experiments are given in Table 3.

Table 3. Modeling result of battery parameters.

Parameter	Experiment I	Experiment II	
		Discharge	Charge
K_0	29.5111	27.0101	28.3471
K_1	−0.0078	0.1242	0.0015
K_2	0.00392	0.0698	1.8381
K_3	0.0847	−0.0016	0.8825
K_4	0.0142	−0.1993	−0.3220
R^+	0.018	0.0818	0
R^-	0.0194	0	0.0795
H	−0.1187	0.6548	−0.5651

Four different estimation methods including the Equip method, the "ECE + EKF" method, the "ECE + UKF" method, and the "Modified ECE + EKF" method are used on the same battery packs for comparisons. The Equip method is measured by the MCF-60L2030A. The "ECE + EKF" method is the ECE method combined with the EKF method. The "ECE + UKF" method is the ECE method combined with the UKF method. The "Modified ECE + ECE" method is a modified ECE method combined with the EKF method.

The initial values of the EKF algorithm used for the state, the state error covariance, the process noise covariance, and the measurement noise covariance for both EKF and UKF algorithms are the same, as shown in Table 4.

Table 4. Initial values of SOC estimation.

Parameter	Quality	Value	Unit
C	nominal capacity	8.4	AH
$\eta_{C/3}$	base coulombic efficiency	0.9982	-
K_S	influence of the SOC on the coulombic efficiency	0.98	-
K_{SD}	self-discharge coefficient	2×10^{-8}	1/second
Cov_0	state error covariance	1	-
Q_w	process noise covariance	10^{-9}	-
R_v	measurement noise covariance	1	-

In Experiment I, the comparison results for the terminal voltage estimation are shown in Figure 10a. Figure 10b, an enlargement of Part A of Figure 10a, shows that the proposed method accurately tracks the real terminal voltage value with an estimation error of less than ±0.1 V in comparison with the other algorithms.

Figure 10. Modeling results in Experiment I. (**a**) Terminal voltage; (**b**) The enlarged Part A of Figure 10a.

(**a**)

(**b**)
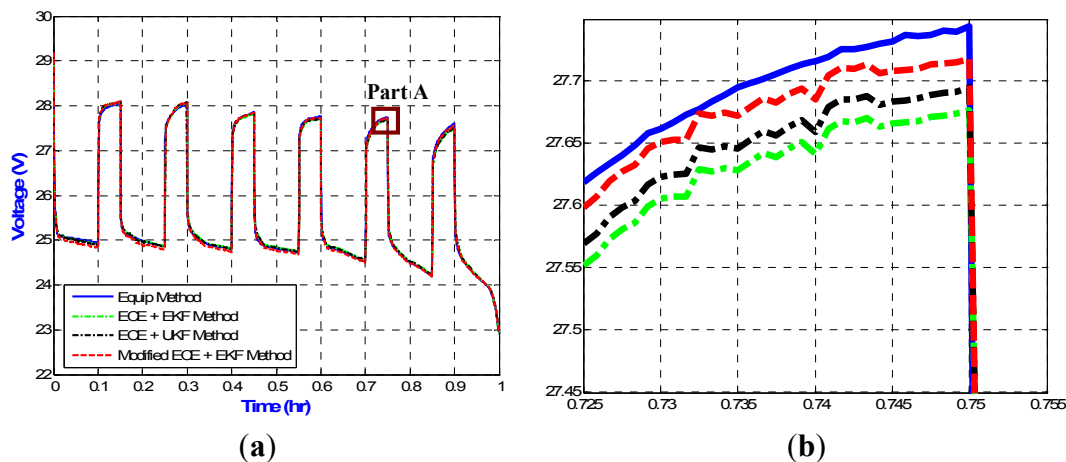
In Experiment II, the results comparing the models of the discharge and charge of the battery pack voltage estimation with the true voltage for the pulsed-current test using those parameters are shown in Figure 11a,b, respectively. From the enlarged view of Figure 11a,b, we can see that the proposed method produces better results than those of other two methods. The results also show that the battery model can represent the battery packs' terminal voltages with respect to discharging and charging currents (with the exception of the relaxation effect in all methods).

Figure 11. Modeling results in Experiment II. (**a**) Discharge; (**b**) Charge.

(**a**)

(**b**)
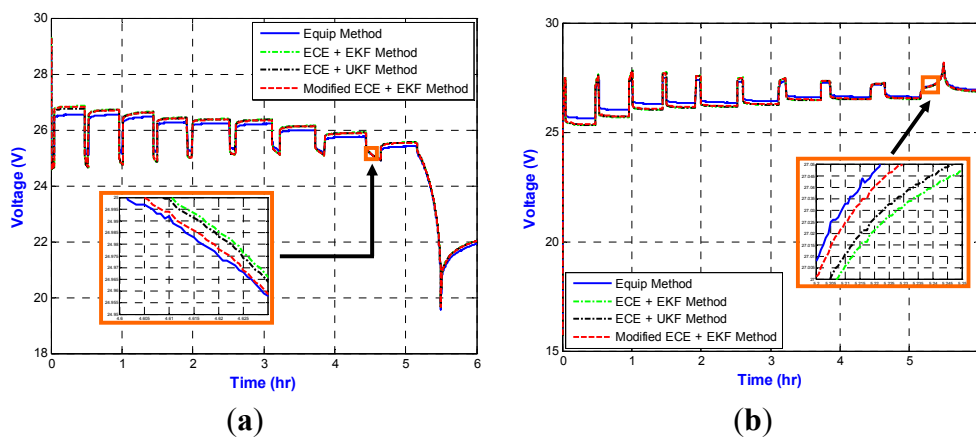
5.5. SOC Estimation Results

The battery pack SOC is estimated from experimental data and from four estimation methods. In Experiment I, the estimation error starts at zero, since the model is correctly initialized in all estimation methods. The comparison results for the SOC estimation are shown in Figure 12a. In Figure 12b, the associated SOC estimation errors are shown to converge to a ±1% error band. The figure also shows that the SOC error of the proposed algorithm can converge closely to zero during discharging. We can adjust the self-discharge coefficient so that the SOC errors converge closely to zero in all intervals, as shown in Figure 13. In Figure 13, the divergence of SOC estimation error is mainly caused by the LabVIEW-based virtual measurement unit. It has 3 second delay when the state

makes transitions (Discharge-to-Charge or Charge-to-Discharge). The mean absolute error (MAE) of the SOC estimation is calculated using the following equation:

$$s_{MAE,N} = \frac{\sum_{j=1}^{N}\left|s_j - \hat{s}_j\right|}{N} \tag{29}$$

where $s_{MAE,N}$ is the MAE for the SOC estimates up to and including time step N and s_j is the experimental SOC at time step j.

Figure 12. SOC estimation in Experiment I (**a**) SOC profile; (**b**) SOC error profile; (**c**) MAE profile.

(a)

(b)

(c)
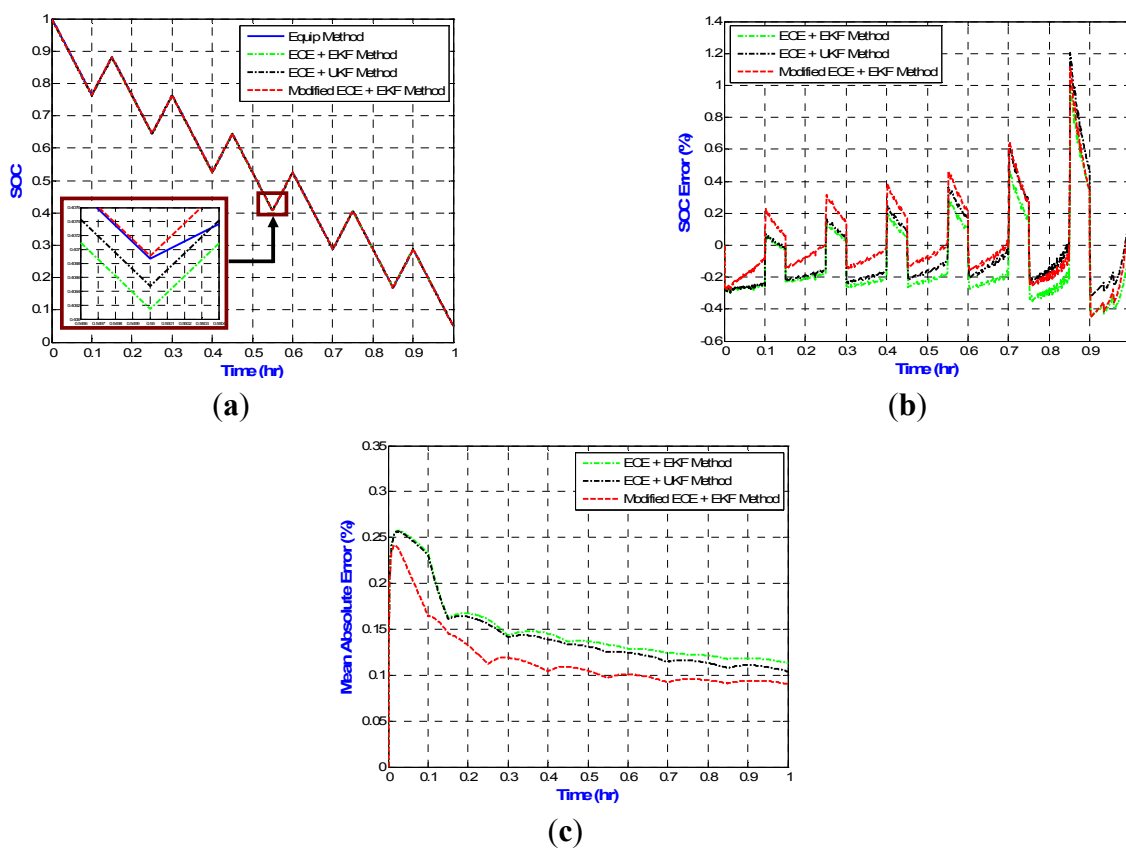
Figure 13. SOC estimation error in Experiment I when the $K_{SD, charge}$ and $K_{SD, discharge}$ are set to 1.97×10^{-7} and 6.09×10^{-8}, respectively.
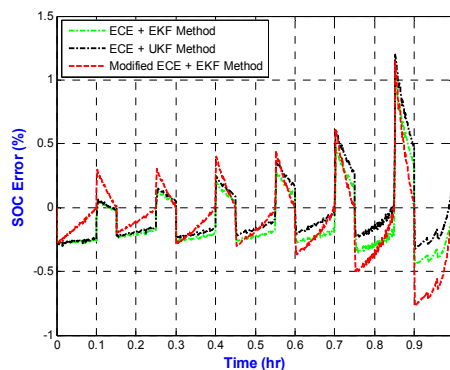
To make them more readable, the results for the MAE of SOC are shown in Figure 12c. It is clear that the proposed algorithm can estimate the battery pack SOC more accurately, compared to the other two algorithms. The advantages of UKF over EKF are that it captures the true mean and covariance more accurately and no need to calculate the Jacobian. It can be shown that the UKF algorithm can give better performance than the EKF algorithm.

In Experiment II, the initial SOC value is set to 0.5 in all estimation methods, so the estimation error starts at ±50% under charge/discharge. This explains why the SOC estimation error is not initially zero in the discharging/charging process of Experiment II.

The comparison results for the SOC estimation under discharge in Experiment II are shown in Figure 14. The associated estimation errors under discharge are shown in Figure 15. It is obvious that the estimation errors of the proposed method under discharge are much smaller than those of other two algorithms. The SOC error of the proposed method converges to 0.16%, while those of other methods are greater than 1%.

Figure 14. SOC estimation under discharge in Experiment II.
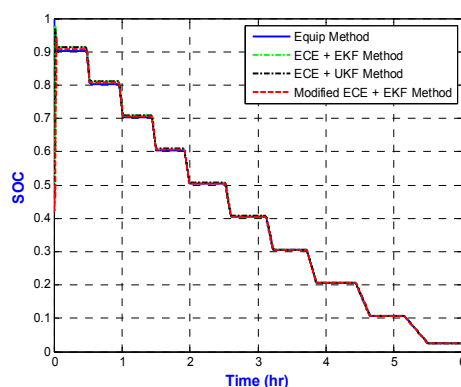
Figure 15. SOC estimation error under discharge in Experiment II.
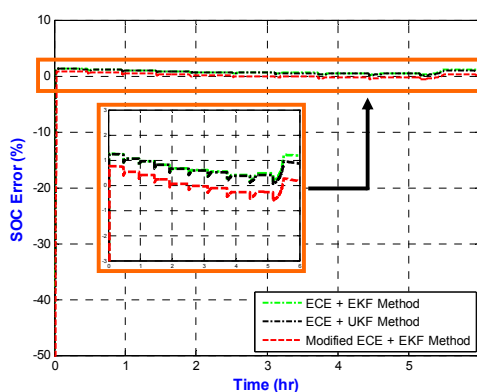
Figure 16 shows a comparison of SOC estimations under charge; the SOC error of the proposed method converges to 0.24%, while those of other methods can reach 1%, as shown in Figure 17. Clearly, the proposed SOC estimator has better performance. Figure 18a,b shows the MAE results under discharge and charge in Experiment II, respectively. The figures show that the proposed method gives a smaller MAE than either of other two methods does.

Figure 16. SOC estimation under charge in Experiment II.
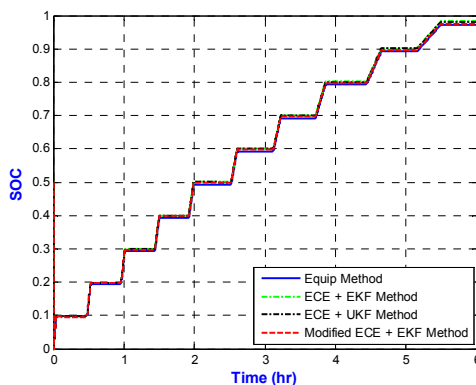
Figure 17. SOC estimation error under charge in Experiment II.
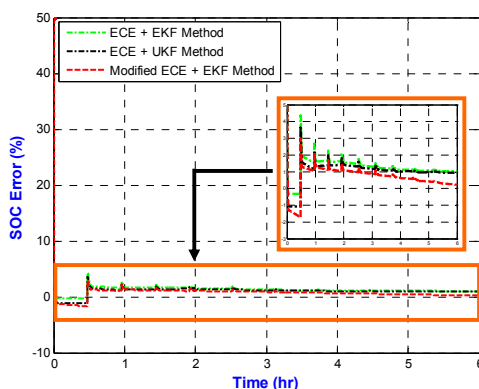
Figure 18. MAE error results in Experiment II. (**a**) Discharge; (**b**) Charge.

(**a**)　　　　　　　　　　　　　　　　(**b**)
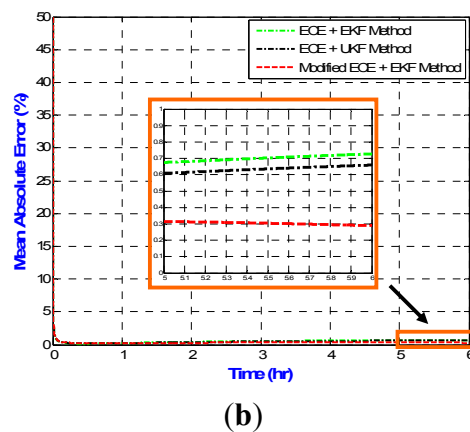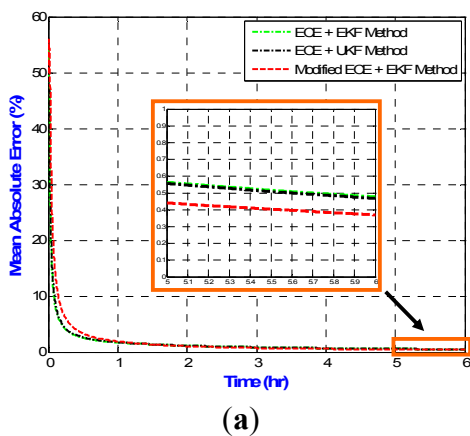
6. Application in Robots

This section demonstrates that a humanoid robot, called Nino, which is being developed by our laboratory performs the model identification and the SOC estimation by considering the proposed algorithm discussed in Section 2 and Section 3. A photograph of the humanoid robot is shown in Figure 19. The humanoid robot has DOFs in its head and hands to achieve facial expressions and grasping motions. In this experiment, we test the proposed algorithm performance while the humanoid robot is set to wave the right and left arms and repeat to run two processes. The current and voltage

profiles for this experiment are shown in Figure 20a,b, respectively. The motors of the humanoid robot are turned on at 46 s. The regions squared in blue dotted line and green solid line in Figure 20b show that the humanoid robot is waving the right and left arms in round 1 and round 2, respectively.

Figure 19. The humanoid robot, Nino.
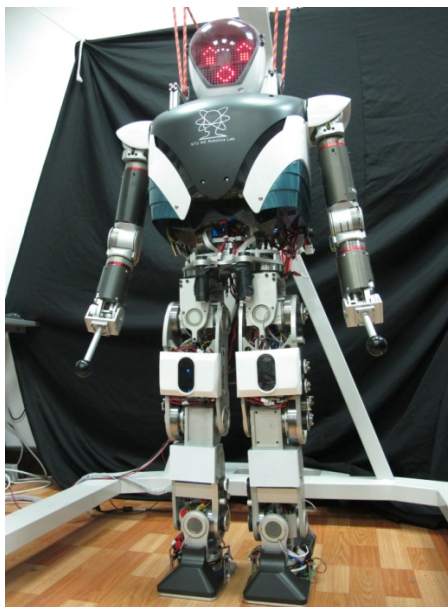
Figure 20. The humanoid robot test. (**a**) Current profile; (**b**) Voltage profile.

(**a**)

(**b**)
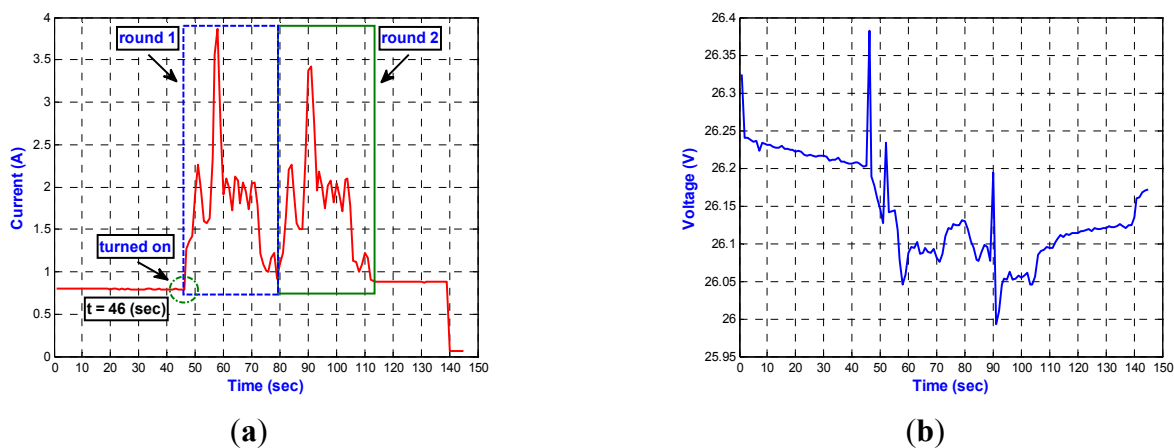
The comparison results for the terminal voltage and voltage error are shown in Figure 21a,b, respectively. From these figures, we can see that the proposed algorithm accurately tracks the real terminal voltage value with an estimation error of less than ±0.05 V except impulses in comparison with the other algorithms. The initial SOC state is set to 0.8. The comparison results for SOC estimation in this experiment are shown in Figure 22a. In Figure 22b, the associated SOC estimation errors in this experiment are shown to converge to a ±0.015% error band. The experimental results show that the SOC estimation results of the proposed algorithm are more accurate and robust than those of other two methods. In addition, we can see that the SOC error graph is similar in shape to the current graph shown in Figure 20a. In this experiment, the average temperature is 25.26 °C when the test begins and 25.23 °C when the test ends.

Figure 21. Modeling results in the humanoid robot test (**a**) Voltage profile; (**b**) Voltage error profile.

(**a**)

(**b**)
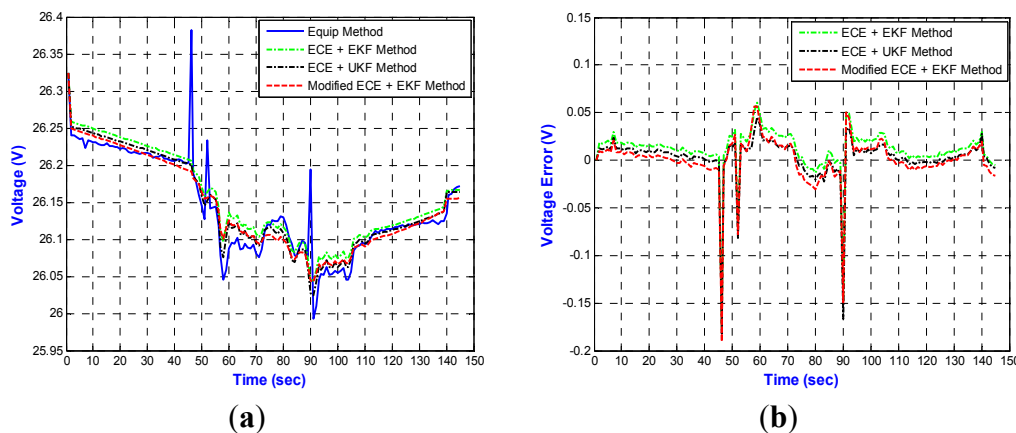
Figure 22. SOC estimation results in the humanoid robot test (a) SOC profile; (b) SOC error profile.

(**a**)

(**b**)
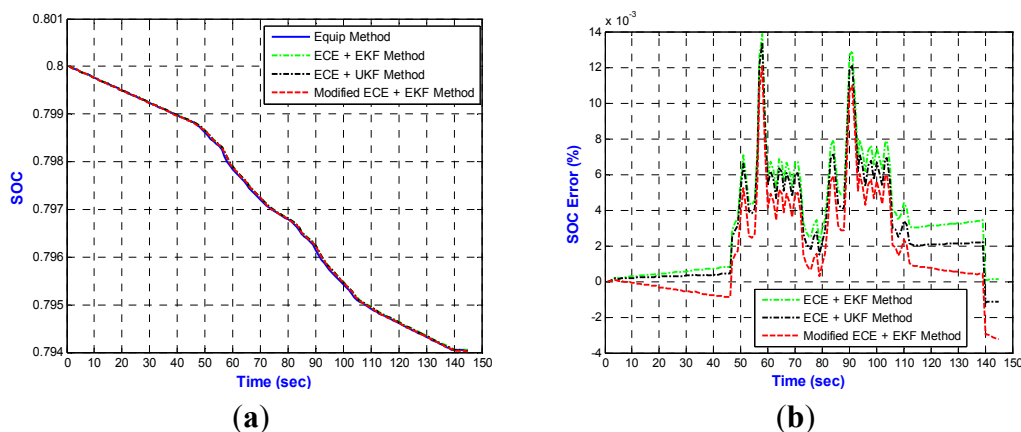
Table 5 summarizes the experimental results of the proposed SOC estimation method in comparison with other SOC estimation algorithms reported in [1,5,10,24,31,32,34,36]. The SOC estimation algorithms in [5,10,32] are off-line results. The SOC estimation error of the proposed method is comparable to [31] but smaller than the remaining methods already presented in the literature. Moreover, from Table 5, it can be noted that the proposed method has the smallest voltage estimation error. Furthermore, the proposed method also considers the hysteresis effect, temperature effect, and self-discharge effect.

Table 5. Comparison with SOC Estimation Algorithm in the literature.

Performance Index	[1]	[5]	[10]	[24,36]	[31]	[32]	[34]	This work
Battery Packs	Yes	Yes	No	Yes	Yes	Yes	Yes	Yes
Battery Type	Ni/MH	Li-Ion	LiFePO$_4$	LiPB	Lead-Acid	Lead-Acid	Li-Ion	LiFePO$_4$
Nominal Capacity (Ah)	80	N.A.	1.1	7.5	45	100	100	8.4
Nominal Voltage (V)	384	N.A.	3.6	3.8	12	8	64	26.4
Initial SOC Value	0.69	0.9	0.5	1	0.45	0.5	0.5	0.5
SOC Estimation Error (%)	2.5	1.5	<2	6.5	<0.12	±1	±1.7	<0.25
Voltage Estimation Error (V)	N.A.	N.A.	N.A.	0.5	N.A.	N.A.	±1	±0.1
On-line/Off-line	On-line	Off-line	Off-line	On-line	On-line	Off-line	On-line	On-line
Hysteresis Effect	Yes	Yes	Yes	Yes	No	Yes	Yes	Yes
Relaxation Effect	No	No	No	No	Yes	No	No	No
Temperature Effect	Yes	Yes	No	No	No	No	No	Yes
Self-Discharge Effect	Yes	No	No	No	No	No	No	Yes
Algorithm	ECE + EKF	ECE + EKF	Adaptive Observer	EKF	UKF	AEKF	AUKF	Modified ECE + EKF

7. Conclusions

In this paper, a novel combined method, denoted as "Modified ECE + EKF", is proposed for SOC estimation of LiFePO$_4$ battery packs. A modified ECE method that considers self-discharge, influence of temperature and SOC on the coulombic efficiency is proposed to estimate the SOC used in robot applications. This approach uses the EKF algorithm to correct the initial value used in the Ah counting method. The zero-state hysteresis correction term is used to depict the hysteresis effect of the battery. The experimental results show that the proposed method is superior to traditional techniques, such as ECE combined with EKF and ECE combined with UKF, giving a SOC estimation within 1% of its true value. In addition, the proposed algorithm is more accurate and robust than those of other two methods.

Acknowledgments

References

1. Wang, J.; Cao, B.; Chen, Q.; Wang, F. Combined state of charge estimator for electric vehicle battery pack. *Control Eng. Pract.* **2007**, *15*, 1569–1576.
2. Dai, H.; Wei, X.; Sun, Z. Online SOC Estimation of High-power Lithium-Ion Batteries Used on HEVs. In Proceedings of the IEEE Conference on Vehicular Electronics and Safety, Beijing, China, 13–15 December 2006; pp. 342–347.

3. Liao, Y.; Huang, J.; Zeng, Q. A novel method for estimating state of charge of lithium ion battery packs. *Adv. Mater. Res.* **2010**, *152–153*, 428–435.

4. Lee, S.J.; Kim, J.H.; Lee, J.M.; Cho, B.H. State-of-charge and capacity estimation of lithium-ion battery using a new open-circuit voltage *versus* state-of-charge. *J. Power Sources* **2008**, *185*, 1367–1373.

5. Liao, C.L.; Li, H.J.; Wang, L.F. A Dynamic Equivalent Circuit Model of LiFePO$_4$ Cathode Material for Lithium Ion Batteries on Hybrid Electric Vehicles. In Proceedings of the IEEE Vehicle Power and Propulsion Conference, Dearborn, MI, USA, 7–11 September 2009; pp. 1662–1665.

6. Chiang, Y.H.; Sean, W.Y. Dynamical Estimation of State-of-Health of Batteries by Using Adaptive Observer. In Proceedings of the 2nd International Conference on Power Electronics and Intelligent Transportation System, Shenzhen, China, 19–20 December 2009; Volume 1; pp. 110–115.

7. Kim, I.S. A technique for estimating the state of health of lithium batteries through a dual-sliding-mode observer. *IEEE Trans. Power Electron.* **2010**, *25*, 783–794.

8. Zhang, H.; Chow, M.Y. Comprehensive Dynamic Battery Modeling for PHEV Applications. In Proceedings of the IEEE Power and Energy Society General Meeting, Minneapolis, MN, USA, 25–29 July 2010; pp. 1–6.

9. Hu, X.S.; Sun, F.C.; Zou, Y. Estimation of state of charge of a lithium-ion battery pack for electric vehicles using an adaptive Luenberger observer. *Energies* **2010**, *3*, 1586–1603.

10. Roscher, M.A.; Sauer, D.U. Dynamic electric behavior and open-circuit-voltage modeling of LiFePO$_4$-based lithium ion secondary batteries. *J. Power Sources* **2011**, *196*, 331–336.

11. Kim, J.; Shin, J.; Jeon, C.; Cho, B. High Accuracy State-of-charge Estimation of Li-Ion Battery Pack based on Screening Process. In Proceedings of the 26th Applied Power Electronics Conference and Exposition, Fort Worth, TX, USA, 17–21 March 2011; pp. 1984–1991.

12. Hu, X.S.; Sun, F.C.; Zou, Y.; Peng, H. Online Estimation of an Electric Vehicle Lithium-Ion Battery Using Recursive Least Squares with Forgetting. In Proceedings of the American Control Conference, San Francisco, CA, USA, 29 June–1 July 2011; pp. 935–940.

13. Schmidt, J.P.; Chrobak, T.; Ender, M.; Illig, J.; Klotz, D.; Ivers-Tiffee, E. Studies on LiFePO$_4$ as cathode material using impedance spectroscopy. *J. Power Sources* **2011**, *196*, 5342–5348.

14. Zhang, Y.; Wang, C.Y.; Tang, X. Cycling degradation of an automotive LiFePO$_4$ lithium-ion battery. *J. Power Sources* **2011**, *196*, 1513–1520.

15. Uno, M.; Tanaka, K. Influence of high-frequency charge-discharge cycling induced by cell voltage equalizers on the life performance of lithium-ion cells. *IEEE Trans. Veh. Technol.* **2011**, *60*, 1505–1515.

16. Szumanowski, A.; Chang, Y.H. Battery management system based on battery nonlinear dynamics modeling. *IEEE Trans. Veh. Technol.* **2008**, *57*, 1425–1432.

17. Gould, C.R.; Bingham, C.M.; Stone, D.A.; Bentley, P. State of Health Estimation of VRLA Batteries Using Fuzzy Logic. In Proceedings of the 18th Iranian Conference on Electrical Engineering, Isfahan, Iran, 11–13 May 2010; pp. 629–634.

18. Chen, Z.; Qiu, S.; Masrur, M.A.; Murphey, Y.L. Battery State of Charge Estimation Based on a Combined Model of Extended Kalman Filter and Neural Networks. In Proceedings of the International Joint Conference on Neural Networks, San Jose, CA, USA, 31 July–5 August 2011; pp. 2156–2163.

19. Guo, G.; Wu, X.; Zhuo, S.; Xu, P.; Xu, G.; Cao, B. Prediction State of Charge of Ni-MH Battery Pack Using Support Vector Machines for Hybrid Electric Vehicles. In Proceedings of the IEEE Vehicle Power and Propulsion Conference, Harbin, China, 3–5 September 2008; pp. 1–4.

20. Bhangu, B.S.; Bentley, P.; Stone, D.A.; Bingham, C.M. Nonlinear observers for predicting state-of-charge and state-of-health of lead-acid batteries for hybrid-electric vehicles. *IEEE Trans. Veh. Technol.* **2005**, *54*, 783–794.

21. Nam, O.; Lee, J.; Lee, J.; Kim, J.; Cho, B.H. Li-ion Battery SOC Estimation Method Based on the Reduced Order Extended Kalman Filtering. In Proceedings of the 4th International Energy Conversion Engineering Conference and Exhibit, San Diego, CA, USA, 26–29 June 2006; pp. 1–9.

22. Vasebi, A.; Partovibakhsh, M.; Bathaee, S.M.T. A novel combined battery model for state-of-charge estimation in lead-acid batteries based on extended Kalman filter for hybrid electric vehicle applications. *Hybrid Electr. Veh.* **2007**, *174*, 30–40.

23. Feng, X.; Sun, Z. A Battery Model Including Hysteresis for State-of-Charge Estimation in Ni-MH. In Proceedings of the IEEE Vehicle Power and Propulsion Conference, Harbin, China, 3–5 September 2008; pp. 1–5.

24. Plett, G.K. Extended kalman filtering for battery management systems of LiPB-based HEV battery packs: Part 2. Modeling and identification. *J. Power Sources* **2004**, *134*, 262–276.

25. Han, J.; Sunwoo, M. Extended Kalman Filtering for State of Charge Estimation of Lead-Acid Batteries. In Proceedings of the International Federation of Automotive Engineering Societies, Munich, Germany, 14–19 September 2008; pp. 1–7.

26. Xu, J.; Gao, M.; He, Z.; Yao, J.; Xu, H. Design and Study on the State of Charge Estimation for Lithium-Ion Battery Pack in Electric Vehicle. In Proceedings of the International Conference on Artificial Intelligence and Computational Intelligence, Las Vegas, NV, USA, 7–8 November 2009; Volume 3; pp. 316–320.

27. He, Z.; Gai, M.; Xu, J. EKF-Ah based State of Charge Online Estimation for Lithium-Ion Power Battery. In Proceedings of the International Conference on Computational Intelligence and Security, Beijing, China, 11–14 December 2009; pp. 142–145.

28. Shi, P.; Zhao, Y.; Shi, P. Application of Unscented Kalman Filter in the SOC Estimation of Li-Ion Battery for Autonomous Mobile Robot. In Proceedings of the IEEE International Conference on Information Acquisition, Weihai, China, 20–23 August 2006; pp. 1279–1283.

29. Zhang, F.; Liu, G.J.; Fang, L.J. Battery State Estimation Using Unscented Kalman Filter. In Proceedings of the IEEE International Conference on Robotics and Automation, Kobe, Japan, 12–17 May 2009; pp. 1863–1868.

30. Santhanagopalan, S.; White, R.E. State of charge estimation using an unscented filter for high power lithium ion cells. *Int. J. Energy Res.* **2010**, *34*, 152–163.

31. Zhang, J.L.; Xia, C.Y. State-of-charge estimation of valve regulated lead acid battery based on multi-state unscented Kalman filter. *Electr. Power Energy Syst.* **2011**, *33*, 472–476.

32. Han, J.; Kim, D.; Sunwoo, M. State-of-charge estimation of lead-acid batteries using an adaptive extended Kalman filter. *J. Power Sources* **2009**, *188*, 606–612.

33. Wang, J.; Guo, J.; Ding, L. An adaptive Kalman filtering based state of charge combined estimator for electric vehicle battery pack. *Energy Convers. Manag.* **2009**, *50*, 3182–3186.

34. Sun, F.C.; Hu, X.S.; Zou, Y.; Li, S. Adaptive unscented Kalman filtering for state of charge estimation of a lithium-ion battery for electric vehicles. *Energy* **2011**, *36*, 3531–3540.

35. Peukert's Law. Available online: http://en.wikipedia.org/wiki/Peukert's_law (accessed on 17 September 2012).

36. Plett, G.K. Extended Kalman filtering for battery management systems of LiPB-based HEV battery packs: part 3. State and parameter estimation. *J. Power Sources* **2004**, *134*, 277–292.

37. Lin, C.; Chen, Q.S.; Wang, J.P.; Huang, W.H.; Wang, Y.C. Improved Ah counting method for state of charge estimation of electric vehicle batteries. *J. Tsinghua Univ.* **2006**, *46*, 247–251.